International Journal on Magnetic Particle Imaging
Vol 9, No 1, Suppl 1, Article ID 2303080, 4 Pages

Infinite Science Publishing

Proceedings Article

A refined debye model for the dynamic magnetization response of superparamagnetic nanoparticles

Sebastian Solibida [a,*] · Dennis Pantke [a] · Franziska Schrank [a] · Volkmar Schulz [a,b,c,d,*]

[a] Department of Physics of Molecular Imaging Systems (PMI), Institute for Experimental Molecular Imaging, RWTH Aachen University, Aachen, Germany
[b] Hyperion Hybrid Imaging Systems GmbH, Pauwelsstrasse 19, 52074 Aachen, Germany
[c] III. Physikalisches Institut B, Otto-Blumenthal-Strasse, 52074 Aachen, Germany
[d] Fraunhofer Institute for Digital Medicine MEVIS, Forckenbeckstrasse 55, Aachen, Germany
[*] Corresponding author, email: {sebastian.solibida;volkmar.schulz}@pmi.rwth-aachen.de

Abstract

Magnetic Particle Imaging (MPI) uses ferrofluids based on superparamagnetic iron-oxide nanoparticles (SPIONs) as a tracer, whose induced voltage in the receive coils is the measured signal. Image reconstruction is often done with the system matrix approach, which needs the signal of a test sample at each position for which the concentration should be reconstructed. In a scanner with a three dimensional reconstruction volume, this measurement becomes very time consuming. Functional parameters such as the temperature might also be reconstructed with a system matrix approach but would require additional system matrices to be measured. Simulation models for the ferrofluid's magnetic behavior might be a solution to this problem, if they are sufficiently fast and precise. Here, we compare the prediction quality and computational cost of the commonly used Debye model with the new Refined Debye model on a viscosity measurement.

I. Introduction

Due to the production process of the SPIONs, the ensemble of SPIONs used in the ferrofluid will contain different sets of physical parameters. For example, the core-diameter and hydrodynamic diameter usually follow a logarithmic-normal distribution [1].
In equilibrium, under a constant external magnetic field $\vec{H}_{ext}$, the expectation value of a SPION's magnetic moment is given by the so-called Langevin function [2]:

$$\vec{m}(\vec{H}_{ext}) = M_s V_c \cdot \left(\coth(x) - \frac{1}{x}\right) \frac{\vec{H}_{ext}}{|\vec{H}_{ext}|};\ x = \frac{|\vec{H}_{ext}|\mu_0 M_s V_c}{k_B T} \quad (1)$$

with the iron-oxide core volume V_c, its saturation magnetization density M_s and temperature T. When $\vec{H}$ is varied, the SPION needs some time to reach the new equilibrium state. The associated time constant is called relaxation time.
A SPION can change the orientation of its magnetic moment by either Neel or Brown relaxation. The former is a internal rotation of the magnetic moment and the latter a rotation of the whole particle due to the Brownian motion of the surrounding medium. Each relaxation type can be described by a stochastic differential equation (SDE) for the magnetic moment, which for a magnetic field of fixed direction can be solved efficiently [3], [4]. Those solutions can be used to determine the relaxation time of the respective relaxation process.
Since in reality both relaxation processes are interdepen-

dent, the two SDEs need to be coupled, which greatly increases the computational cost of a numeric solution. The commonly used Debye model describes the SPION's magnetic moment with the following ordinary differential equation (ODE) [2]:

$$\frac{\mathrm{d}}{\mathrm{dt}}\vec{m}(t) = -\frac{\vec{m}(t) - \vec{m}_{\mathrm{eq}}(t)}{\tau}, \tag{2}$$

which can be rewritten in Fourier space to the computationally cheaper equation

$$\vec{\hat{m}}(\omega) = \mathscr{F}(\vec{m}_{eq})(\omega) \cdot \frac{1}{1 + i\omega\tau}, \tag{3}$$

with $\vec{m}_{eq}$ being the magnetic moment in equilibrium defined in (1) and τ the relaxation time of the SPION calculated from the zero-field relaxation times τ_B and τ_N as $\frac{1}{\tau} = \frac{1}{\tau_B} + \frac{1}{\tau_N}$. τ_B resp. τ_N is the time in which aligned magnetic moments decay when no external magnetic field and only Brownian motion or Neel rotation is present [5]. To account for the aforementioned parameter variances in a ferrofluid, a ferrofluid simulation model might sample the expected variances and simulate different sets of SPIONs with its SPION simulation model. This is not always the case, especially when the Debye model is used. In this work, we will present a ferrofluid simulation model that bases its SPION simulation on a modified version of equation (2).

II. Methods and materials

Refined Debye Model: Analog to the Debye model the ODE of the Refined Debye model (RDM) reads:

$$\frac{\mathrm{d}}{\mathrm{dt}}\vec{m}(t) = -\frac{\vec{m}(t) - \vec{m}_{eq}(t)}{\tau(t)} \tag{4}$$

The newly introduced time dependence of τ eliminates the simple solution in Fourier space seen in the Debye model. It can be chosen whether the time dependence of the relaxation-time only comes from the external fields amplitude or from its derivative as well. Note that both the assumption of a time-dependent τ and the form of its time-dependence is purely heuristic. In the first case, this leads to

$$\frac{1}{\tau(t)} = \frac{1}{\tau_N(|\vec{H}_{ext}(t)|)} + \frac{1}{\tau_B(|\vec{H}_{ext}(t)|)} \tag{5}$$

and in the second

$$\frac{1}{\tau(t)} = \frac{W(|\vec{H}_{ext}|, |\frac{\mathrm{d}\vec{H}_{ext}}{\mathrm{dt}}|)}{\tau_N(|\vec{H}_{ext}|)} + \frac{1 - W(|\vec{H}_{ext}|, |\frac{\mathrm{d}\vec{H}_{ext}}{\mathrm{dt}}|)}{\tau_B(|\vec{H}_{ext}|)} \tag{6}$$

The zero-field relaxation times $\tau_{B/N}$ of the Debye model have been replaced with the field-dependent relaxation times $\tau_{B/N}(|\vec{H}_{ext}(t)|)$, that depend on the absolute value of the externally applied magnetic field $\vec{H}_{ext}$. Contrary to the Debye model, these relaxation times are calculated using the special case solutions for the SDEs of the respective process for a magnetic field that is set from 0 to $|\vec{H}_{ext}|$, as done in [5].

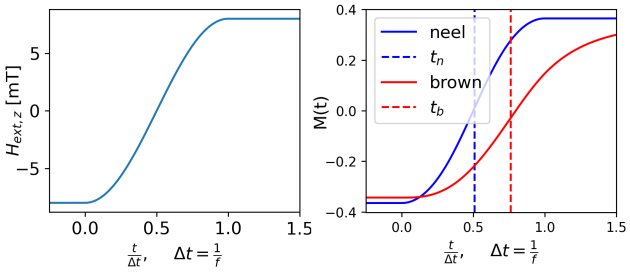

Figure 1: Left: the applied magnetic field. Right: the solution of the decoupled SDE for each process with highlighted inflection point at t_b resp. t_n.

Equation (6) introduces the weighting factor W, for which the results of the special case solutions for the SDEs of the respective process are compared with each other. For this, the external magnetic field is flipped from $-|\vec{H}_{ext}|$ to $|\vec{H}_{ext}|$ in the time $\Delta t = \frac{2|\vec{H}_{ext}|}{|\frac{d}{dt}\vec{H}_{ext}|}$, where a half sine-wave is inserted, see Fig. 1. The time point $t_{b/n}$ at which the change of the magnetic moments absolute value was biggest as well as this value $M'(t_{b/n})$ itself is determined for each process and combined into the weighting factor:

$$W\left(|\vec{H}_{ext}|, \left|\frac{\mathrm{d}\vec{H}_{ext}}{\mathrm{dt}}\right|\right) = \frac{t_b}{t_b + t_n} \cdot \frac{|M'(t_n)|}{|M'(t_n)| + |M'(t_b)|} \tag{7}$$

The ferrofluid simulation model that uses the RDM will always assume a log-normal distributed core-diameter, as this distribution is most common for SPION core diameters.

The benchmark measurement for the ferrofluid simulation models was performed with the multi-frequency-MPI (mf-MPI) developed at the PMI in Aachen [6]. This MPI device is capable of measuring the usually discarded first harmonic of the voltage signal and can be operated at various drive field frequencies and amplitudes. It offers a one-dimensional scanner volume. The measurement used SHP-20 nanoparticles (Ocean NanoTech LLC, San Diego) that were suspended in water-glycerol mixtures with viscosities of 1,2,4,8 and 12 mPas respectively. The drive field was set to 5 kHz at 9 mT. For the fit, only the 1, 2 and 8 mPas data was used.

Four different ferroluid simulation models were tested: one based on the Debye model with only a single set of SPION parameters (**A**), one with an additional log-normal distributed core-diameter (**B**). The RDM was tested with (**C**) and without the weighting factor (**D**).

Fitted model parameters are the core-diameter d_c (and the width σ_{d_c} of the log-normal distribution for **B**, **C** and

D), the hydrodynamic diameter d_h, the anisotropic energy density K [J/m³/T] and the concentration ρ. The saturation magnetization was fixed to 878 kJ/m³/T .
For comparison of the model performance, all models got their parameters fitted to best describe the measurement. This was done using a differential evolution algorithm [7] using the loss L

$$L = \sum_i |\ln(|\alpha_i|) - \ln(|a_i|)| \tag{8}$$

between the measured harmonics of the voltage signal α_i and the simulated ones a_i. This loss ensures that each harmonic gets weighted equally, as the logarithm only depends on the relative value of $\left|\frac{\alpha_i}{a_i}\right|$.

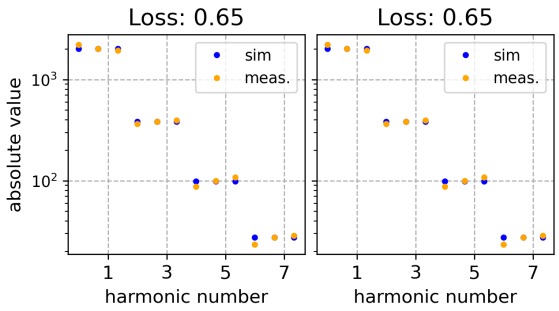

Figure 2: Fit result. Left: model **A**. Right: model **B**. The measurement is shown in yellow. For each harmonic three data points are shown, representing the viscosities 1, 2 and 8 mPas from left to right.

III. Results and Discussion

In Fig. 3, we can see that the absolute value of the measured first harmonic decreases with increasing viscosity, but the higher harmonics show the opposite behavior. The Debye model based simulations **A** and **B** seen in Fig. 2 show no dependence on the viscosity. This is a consequence of equation (3) and the fact that the zero field Brownian relaxation-time $\tau_B = \frac{3\eta V_h}{k_b T}$ monotonously rises with rising viscosity η. As τ_N is independent of η, τ will also monotonously rise with viscosity. The time-derivative of $\vec{m}$ is proportional to the induced voltage, so that the absolute value of the simulated harmonics will be proportional to $\left|\mathcal{F}(\vec{m}_{eq})\frac{i\omega}{1+i\omega\tau}\right|$. This function is monotonously decreasing for τ. But as the measurement showed both an increase and decrease of the absolute harmonic value with rising viscosity, the fit resulted in a viscosity independent result.
The RDM based simulations seen in Fig. 3 manage to qualitatively describe the behavior of the measurement. The RDM's fit quality does only slightly benefit from the weighting factor.
The runtimes of the different models can be seen in Table 1. The weighting factor slows the RDM simulation down by a factor of 20, while giving no meaningful improvement in the description of the measurement. Therefore, the RDM without weighting factor should be the preferred version of the RDM.
When comparing to the speed of a real world measurement, the simulation is run on 10 cores of a AMD Ryzen 3900X, as such a performance level can easily be achieved for each scanner, and the acquisition time for a real world measurement per position is assumed to be one second. The simulation of a single position is a single core workload, but parallelization can be used when multiple positions are requested. It turns out that in this case the RDM with weighting factor would be a little slower than a full measurement based reconstruction, whereas the preferred version of the RDM will be more than 10 times faster.

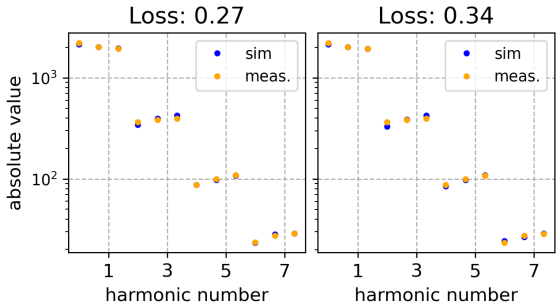

Figure 3: Fit result. Left: model **C**. Right: model **D**. The measurement is shown in yellow. For each harmonic three data points are shown, representing the viscosities 1, 2 and 8 mPas from left to right.

The two Debye based simulations are all at least a factor of 10 faster than any version of the RDM, therefore both are faster than a measurement based reconstruction.
The excitation with the mf-MPI is 1D, but the RDM is ready to be used on 3D excitations and its performance there is not investigated yet.
In both the Debye model and the RDM only the absolute value of the anisotropy-axis is used while its direction is fixed to the z-aixs. In reality the easy axis will rotate during excitation and the resulting effects on the particle signal can not be mapped with any of the two simualtion models.

Table 1: Runtime comparison.

Model	**A**	**B**	**C**	**D**
One entry [s]	0.01	0.1	20	1
1000 entries [min]	$\frac{1}{60}$	$\frac{1}{6}$	80	2

10.18416/ijmpi.2023.2303080

IV. Conclusion

This paper shows that a ferrofluid simulation model based on the newly introduced RDM is able to qualitatively describe a viscosity measurement series using SHP-20. The RDM is an improvement over the Debye model in this case, as the latter is mathematically unable to describe the behavior of the harmonics for different viscosities. When the weighting factor is not used, the RDM is a viable option for system matrix simulation, as it outperforms a full measurement based approach when using multi-threading on an AMD Ryzen 3900X.

Acknowledgments

We thank Pauline Kreft for the preparation of the SPION samples.
Research funding: We acknowledge the financial support by the German research foundation (DFG, grant number SCHU 2973/5-1).

Author's statement

Conflict of interest: Authors state no conflict of interest.

Supplements

The code for the RDM simulation can be found at https://git.rwth-aachen.de/sebastian.solibida/mpi-simulation.

References

[1] I. J. Bruvera, P. Mendoza Zélis, M. Pilar Calatayud, G. F. Goya, and F. H. Sánchez. Determination of the blocking temperature of magnetic nanoparticles: The good, the bad, and the ugly. *Journal of Applied Physics*, 118(18):184304, 2015, doi:10.1063/1.4935484.

[2] T. Knopp and T. M. Buzug, Magnetic Particle Imaging: An Introduction to Imaging Principles and Scanner Instrumentation. Berlin/Heidelberg: Springer, 2012, doi:10.1007/978-3-642-04199-0.

[3] H. Rogge, M. Erbe, T. M. Buzug, and K. Lüdtke-Buzug. Simulation of the magnetization dynamics of diluted ferrofluids in medical applications. *Biomedizinische Technik/Biomedical Engineering*, 58(6):601–609, 2013, doi:10.1515/bmt-2013-0034.

[4] H. Albers, T. Kluth, and T. Knopp. Simulating magnetization dynamics of large ensembles of single domain nanoparticles: Numerical study of brown/néel dynamics and parameter identification problems in magnetic particle imaging. *Journal of Magnetism and Magnetic Materials*, 541:168508, 2022, doi:10.1016/j.jmmm.2021.168508.

[5] R. J. Deissler, Y. Wu, and M. A. Martens. Dependence of brownian and néel relaxation times on magnetic field strength. *Medical Physics*, 41(1):012301, 2014, doi:10.1118/1.4837216.

[6] D. Pantke, N. Holle, A. Mogarkar, M. Straub, and V. Schulz. Multifrequency magnetic particle imaging enabled by a combined passive and active drive field feed-through compensation approach. *Medical Physics*, 46(9):4077–4086, 2019, doi:10.1002/mp.13650.

[7] scipy implementation of a differential evolution algorithm. (), URL: https://docs.scipy.org/doc/scipy/reference/generated/scipy.optimize.differential_evolution.html#scipy-optimize-differential-evolution.

